Two-dimensional electron systems beyond the diffusive regime

P. Markoš
Department of Physics, FEI, Slovak University of Technology, 812 19 Bratislava, Slovakia
(Received 3 May 2010; published 24 September 2010)

Transport properties of disordered electron system can be characterized by the conductance, Lyapunov exponent, or level spacing. Two additional parameters, K_{11} and γ were introduced recently which measure the nonhomogeneity of the spatial distribution of the electron inside the sample. For the orthogonal, unitary, and symplectic two-dimensional disordered models, we investigate numerically the system-size dependence of these parameters in the diffusive and localized regimes. Obtained size and disorder dependence of K_{11} and γ is in agreement with single parameter transport theory. In the localized regime, $\gamma \to 0$ independently of the physical symmetry of the model. In the diffusive regime, γ equals to the symmetry parameter β. For the symplectic model we analyze the size dependence of γ in the critical region of the metal-insulator transition and found the nonuniversal critical value γ_c.

DOI: 10.1103/PhysRevB.82.094203 PACS number(s): 71.30.+h, 73.23.−b, 72.10.−d

I. INTRODUCTION

Transport of electrons through disordered structures offers a broad variety of interesting universal phenomena.[1,2] With increase in the strength of the disorder the character of the transport changes from the ballistic to diffusive up to the insulating, where all electrons are localized.[3]

In the limit of weak disorder (diffusive regime) the transport can be studied analytically using, for instance, the Dorokhov Mello Pereyra Kumar (DMPK) equation,[4] the Green's-function analysis,[5] or random matrix theory.[6,7] The existence of the metal-insulator transition in two-dimensional (2D) and three-dimensional (3D) models[8,9] is a strong motivation to construct an analytical theory of the transport beyond the diffusive regime.[10,11] Also, numerical data for the localized regime[12–16] show that, contrary to theoretical expectation, the distribution of the logarithm of the conductance is never Gaussian for disordered systems in higher dimension. Therefore, a general transport theory must explain how the dimension of the system and physical symmetry of the model[9] influence the ability of electron to move through the sample.

The most elaborated analytical description of the transport in strongly disordered structures is based on the generalized DMPK equation (GDMPKE).[17] The theory takes into account that the spatial distribution of electrons in the regime of localization is not homogeneous. The last was confirmed by numerical simulations in Refs. 14 and 18. In GDMPK, the nonhomogeneity of electron distribution is measured by a large number of parameters K_{ab} (defined later); however, only two of them, K_{11} and $\gamma = 2K_{12}/K_{11}$ are decisive for the transport.[19]

The GDMPKE is not exactly solvable, but approximate analytical solution for 3D disordered systems[19–21] agrees very well with numerical data. Numerical solution of GDMPKE (Ref. 22) confirmed that it correctly describes disordered orthogonal systems and that parameters K_{ab} depend on the dimension of the system.

Detailed numerical analysis of parameters K_{11} and γ in three-dimensional model was performed in Ref. 20. The aim of this paper is to investigate how these parameters depend on the physical symmetry in 2D models. We present numerical data for the parameters K_{11} and γ for the orthogonal (O) model, unitary (U) and two symplectic (S) (Refs. 23 and 24) models in diffusive and insulating regimes. For the S models, we also study the behavior of both parameters in the critical regime of the metal-insulator transition.

II. GENERALIZED DMPK EQUATION

Consider a disordered system of the length L_z connected to two semi-infinite ideal leads with N open channels. Transmission parameters are given by the transfer matrix, which can be written in general form as[4]

$$T = \begin{pmatrix} u & 0 \\ 0 & u' \end{pmatrix} \begin{pmatrix} \sqrt{1+\lambda} & \sqrt{\lambda} \\ \sqrt{\lambda} & \sqrt{1+\lambda} \end{pmatrix} \begin{pmatrix} v & 0 \\ 0 & v' \end{pmatrix}. \tag{1}$$

In Eq. (1), u and v are $N \times N$ matrices and λ is a diagonal matrix with positive elements $\lambda_a, a = 1, 2, \ldots, N$. In systems with time-reversal symmetry, matrices u' and v' can be represented in terms of u and v.[25] For the orthogonal system, $u' = u^*$ and $v' = v^*$. For the symplectic symmetry, the scattering depends on the spin of the electron; the elements of matrices u and v are 2×2 matrices which fulfill the symmetry relations[6,25]

$$u' = k u^* k^T, \quad v' = k v^* k^T, \quad k = \begin{pmatrix} 0 & -1 \\ 1 & 0 \end{pmatrix}. \tag{2}$$

Statistical variables u, v, and λ contain entire information about the transport. In the weak-disorder limit,[4] the conductance g (in units of $2e^2/h$) is completely determined by eigenvalues λ_a.[6,26]

$$g = \sum_{a=1}^{N} \frac{1}{1+\lambda_a} = \sum_{a=1}^{N} \frac{1}{\cosh^2 x_a/2}. \tag{3}$$

In the last equation, we used the parametrization $\lambda_a = (\cosh x_a - 1)/2$.

The probability distribution of λ's can be found as a solution of the DMPK equation.[4] The generalization of the DMPK for the orthogonal symmetry class was done by Mut-

talib and Klauder[17] who introduced new parameters, K_{ab} which characterize the spatial distribution of the electron in the disordered sample. The generalized DMPK equation reads[17]

$$\frac{\partial p_{L_z}(\lambda)}{\partial(L_z/\ell)} = \frac{1}{J}\sum_a^N \frac{\partial}{\partial\lambda_a}\left[\lambda_a(1+\lambda_a)K_{aa}J\frac{\partial p}{\partial\lambda_a}\right], \tag{4}$$

where ℓ is the mean free path, and

$$J \equiv \prod_{a<b}^{N} |\lambda_a - \lambda_b|^{\gamma_{ab}}, \quad \gamma_{ab} \equiv \frac{2K_{ab}}{K_{aa}}. \tag{5}$$

This equation can be simplified when all K_{aa} are approximated by K_{11} and $\gamma_{ab} \approx \gamma$ for all a, b $(a \neq b)$. This approximation was confirmed by numerical work.[20,22]

Although the conductance is still given by Eq. (3), it becomes implicitly a function of the spatial distribution of the electron.

III. MODELS

In numerical work, disordered sample is represented by 2D square disordered lattice of the size $L \times L$. The orthogonal 2D model with on-site disorder is defined by the Hamiltonian

$$\mathcal{H} = W\sum_{xz} \epsilon_{xz} c_{xz}^\dagger c_{xz} + V_\perp \sum_{xz} c_{x+a,z}^\dagger c_{xz} + c_{xz}^\dagger c_{x+a,z} + V_\parallel \sum_{xz} c_{x,z+a}^\dagger c_{xz} + c_{xz}^\dagger c_{x,z+a}. \tag{6}$$

Here, a is the lattice spacing, ϵ_{xz} are random energies from the box distribution, $|\epsilon_{xz}| < 1/2$, W measures the strength of the disorder, and $V_\parallel \equiv 1$ defines the energy scale. To avoid closed channels in leads, we use $V_\perp / V_\parallel = t < 1$.[27] In what follows we consider $t=0.9$, the energy of the electron $E=0.01$. With $a \equiv 1$, we identify the number of channels

$$N \equiv L. \tag{7}$$

It is generally accepted[2,8] that only localized regime exists in the model when the size of the system $L \to \infty$ (the critical disorder $W_c = 0$). Nevertheless, diffusive transport is observable for sufficiently weak disorder and small sample size.[13]

The second model of interest is the symplectic model with spin-dependent hopping. Here, the hopping of electron from one site to the neighboring one can be accompanied by the change in the sign of the spin and $V_\parallel$ and $V_\perp$ become 2×2 matrices. In numerical simulations, we study the Ando model with hopping terms

$$V_\perp = t\begin{pmatrix} V_1 & -V_2 \\ V_2 & V_1 \end{pmatrix}, \quad V_\parallel = \begin{pmatrix} V_1 & -iV_2 \\ -iV_2 & V_1 \end{pmatrix}. \tag{8}$$

The spin-orbit coupling is characterized by the parameters $S = V_1$ and $V_1^2 + V_2^2 = 1$. In this paper, $S = 0.5$. We also study the Evangelou-Ziman (EZ) model[23] which uses the random hopping matrices V: with help of three independent random variables, t^x, t^y, t^z, distributed uniformly in interval $(-\mu/2, \mu/2)$

$$V_\perp = V_{xz,x+az} = t\begin{pmatrix} 1+it^z & -t^y+it^x \\ t^y - it^x & 1-it^z \end{pmatrix} \tag{9}$$

and

$$V_\parallel = V_{xzxz+a} = \begin{pmatrix} 1+it^z & -t^y+it^x \\ t^y - it^x & 1-it^z \end{pmatrix}, \tag{10}$$

and consider $\mu = 1$.

Both Ando and EZ models exhibit the metal-insulator transition when the disorder W reaches the critical value W_c.[23,24] Owing to the anisotropy of our models, the critical disorder differs from that obtained in previous works.[23,28] We found $W_c \approx 5.525$ for the Ando model and $W_c = 6.375$ for the EZ model.

The 2D model with external magnetic field B can be obtained by including the Peierls hopping term $V_\perp = t \exp ix\alpha$, $\alpha = (e/\hbar)Ba^2$ into Hamiltonian (6).

IV. MATRIX K

The matrix K_{ab} is defined in terms of higher moments of the matrices v

$$K_{ab} \equiv \langle k_{ab} \rangle. \tag{11}$$

Here, $\langle \cdots \rangle$ represents an ensemble average.

For the orthogonal system, the matrix k_{ab}^{O} is defined as[17]

$$k_{ab}^{\mathrm{O}} = \sum_{\alpha=1}^{L} |v_{\alpha a}|^2 |v_{ab}|^2. \tag{12}$$

In the diffusive regime,[4]

$$K_{ab}^{\mathrm{O}} = \frac{1+\delta_{ab}}{L+1}. \tag{13}$$

For the unitary models,

$$k_{ab}^{\mathrm{U}} = \sum_{\alpha=1}^{L} |v_{\alpha a}|^2 |v'_{ab}|^2 \tag{14}$$

and

$$K_{ab}^{\mathrm{U}} = \frac{1}{L}. \tag{15}$$

For the systems with symplectic symmetry the matrix k_{ab}^{S} is given[29,30]

$$k_{ab}^{\mathrm{S}} = \sum_{\alpha=1}^{L} v_{\alpha a}^\dagger v_{ab}^* \bar{v}_{\alpha b} v_{\alpha_a}. \tag{16}$$

In this equation, the 2×2 matrices $v^\dagger$, v^*, and $\bar{v}$ are defined in terms of the matrix v

$$v = \begin{pmatrix} v_{11} & v_{12} \\ v_{21} & v_{22} \end{pmatrix}, \quad v^\dagger = \begin{pmatrix} v_{11}^* & v_{21}^* \\ v_{12}^* & v_{22}^* \end{pmatrix} \tag{17}$$

and

$$v^* = \begin{pmatrix} v_{11}^* & v_{12}^* \\ v_{21}^* & v_{22}^* \end{pmatrix}, \quad \bar{v} = \begin{pmatrix} v_{22} & -v_{12} \\ -v_{21} & v_{11} \end{pmatrix}. \tag{18}$$

In the diffusive regime, K_{ab}^{S} is degenerated diagonal matrix[29] with diagonal elements

$$K_{ab}^{S} = \frac{2 - \delta_{ab}}{2L - 1}. \tag{19}$$

Our numerical results discussed in Sec. V confirm that the same holds for any disorder strength.

From Eqs. (13), (15), and (19) it follows that

$$\sum_b K_{ab}^{O} = \sum_b K_{ab}^{U} = \sum_b K_{ab}^{S} = 1. \tag{20}$$

We use these relations to test the numerical accuracy of our results.

V. RESULTS

We consider square samples of the size $L \times L$ attached to two semi-infinite ideal leads. The size L increases from $L=10$ to $L=256$ (S model) up to $L=600$ (O model). For each value of L and W, we analyze the statistical ensemble of typically $N_{\text{stat}} \sim 10^4$ samples ($N_{\text{stat}} \sim 1000-4000$ for the largest system size). In numerical calculation, the sample and leads are represented by the $2N \times 2N$ transfer matrices M and M_0, respectively.[31] Following,[32] the conductance is given as a trace of matrices $L^+ M R^+$ and $L^- M R^-$, where R^{+-} (L^{+-}) are $N \times 2N$ ($2N \times N$) matrices composed of right and left eigenvalues of M_0, respectively. The upper index $^+$ ($^-$) indicates the direction of the propagation through the sample. Comparing with Eq. (1) we find

$$L^+ M R^+ = v(1+\lambda)^{-1} v^\dagger \tag{21}$$

and

$$L^- M R^- = v'^\dagger (1+\lambda)^{-1} v'. \tag{22}$$

Thus, eigenvalues λ_a can be obtained numerically by diagonalizing of the matrices $L^+ M R^+$ and $L^- M R^-$. Matrices v and v' consist of corresponding eigenvectors. Details of numerical method are given in Ref. 20. Mean values, K_{11} and K_{12} were calculated as an average over the statistical ensemble

$$K_{ab} = \frac{1}{N_{\text{stat}}} \sum_{i=1}^{N_{\text{stat}}} k_{ab}^{(i)}. \tag{23}$$

Obtained data for k_{ab} were also used for the calculation of probability distributions.

As noted in Sec. IV, K_{ab}^{S} are 2×2 matrices. Numerical data confirm that, with the relative accuracy of 10^{-3}, these matrices remain diagonal degenerate for each value of the disorder and all size of the system.

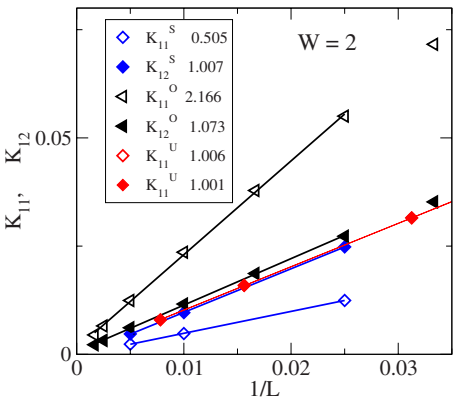

FIG. 1. (Color online) K_{11} and K_{12} as a function of the system size for square lattice $L \times L$ for the S, O, and U systems. The disorder $W=2$. Solid lines are linear fits with slopes given in the legend.

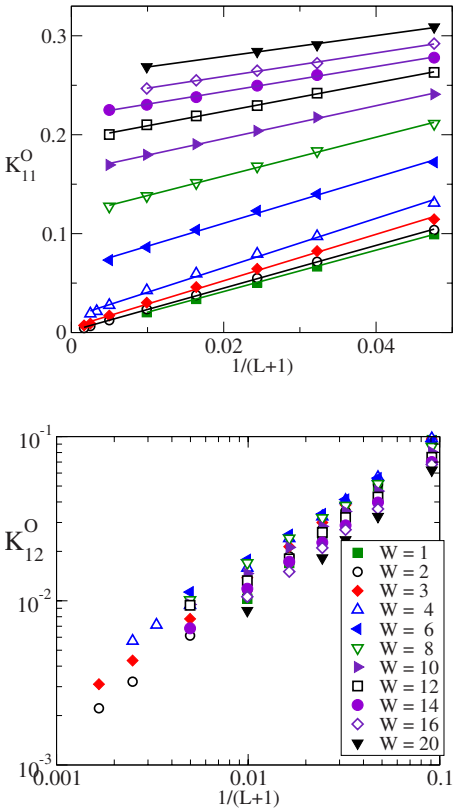

FIG. 2. (Color online) The size dependence of K_{11} (top) and K_{12} (bottom) for the 2D orthogonal model for various strength of the disorder (given in the legend of bottom panel). K_{11} converges to the nonzero limit when $L \to \infty$ for each disorder strength. This limiting value, however, is too small to be observable numerically for weak disorder within the considered size of the system. K_{12} decreases to zero for any value of the disorder W.

A. Diffusive regime

We first verify the prediction of the DMPK equation for the diffusive regime. In Fig. 1 we show the L dependence of parameters K_{11} and K_{12} for the orthogonal and symplectic systems with disorder $W=2$. The system is in the diffusive regime (the conductance g varies between 4.9 and 5.03 for the orthogonal model, and increases from 7 to 11 for the S model). Linear fits shown by solid lines confirm that both K_{11} and $K_{12} \sim 1/L$ and γ equals to the symmetry parameter β

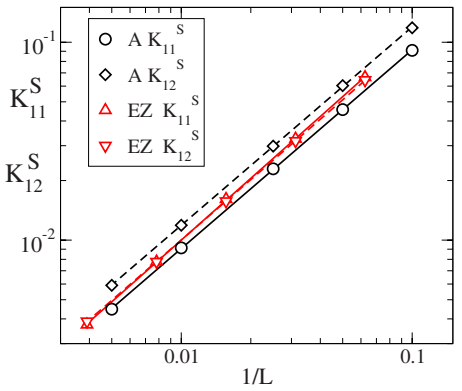

FIG. 3. (Color online) The size dependences K_{11} and K_{12} at the critical point for the symplectic (Ando and EZ models) models. Solid and dashed lines are power fits $K_{1a} \propto L^{-\alpha}$ $(a=1,2)$ with the exponent $\alpha \approx 1.003-1.005$.

in the diffusive regime. The spatial distribution of electrons is homogeneous and no additional parameter must be introduced into the model. The transport is universal, the only model parameter in the DMPK is the ratio L_z/ℓ of the system length to the mean free path. Although the DMPK was derived only for the quasi-one-dimensional systems, our data show that relations in Eqs. (13), (15), and (19) are valid also for the square samples.

B. Insulating regime

In the limit of strong disorder, we expect that K_{aa} depend on the index a and $K_{aa} \sim O(1)$. Contrary, off-diagonal elements K_{ab}, $a \neq b$, should decrease to zero, $K_{ab} \sim 1/L$ $(a \neq b)$ so that $\gamma \sim 1/L$ decreases to zero when the size of the system increases.[17]

Figure 2 shows the L dependence of K_{11}^{O} and K_{12}^{O} for orthogonal systems with various strength of the disorder. Similarly to the 3D orthogonal model discussed in Ref. 20, both K_{11}^{O} and K_{12}^{O} are linear functions of $1/(L+1)$, Since no metallic regime exists for the nonzero disorder, we expect that K_{11}^{O} converges to the nonzero value in the limit of $L \to \infty$ for all values of W

$$K_{11}^{\mathrm{O}} = K_{11}^{\mathrm{O}\infty} + \frac{c}{L+1}. \tag{24}$$

The limiting value $K_{11}^{\mathrm{O}\infty}$ can be easily calculated numerically for strong disorder. This is more difficult for weak disorder $(W<4)$, since $K_{11}^{\mathrm{O}\infty}$ becomes smaller than the inverse of the accessible sample size.

Similar data (not shown) were obtained also for the symplectic models.

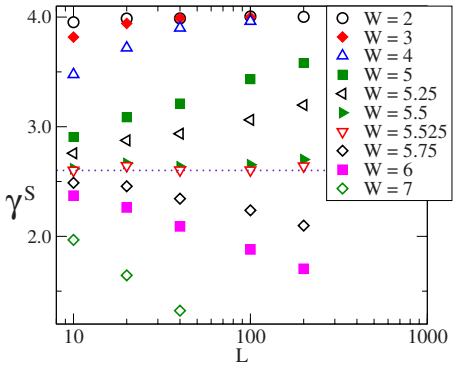

FIG. 4. (Color online) The size dependence of the parameter $\gamma^{\mathrm{S}}=2K_{12}^{\mathrm{S}}/K_{11}^{\mathrm{S}}$ for the Ando model. In the metallic regime, $(W<W_c=5.525)$, γ^{S} slowly increases when L increases and converges to its isotropic value $\gamma^{\mathrm{S}}=4$. In the localized regime $(W>W_c=5.525)$, γ^{S} decreases to zero when the size of the system increases. At the critical point, γ^{S} does not depend on L. The L-independent critical value of $\gamma^{\mathrm{S}} \approx 2.60$ (dotted line) is plotted by dotted line.

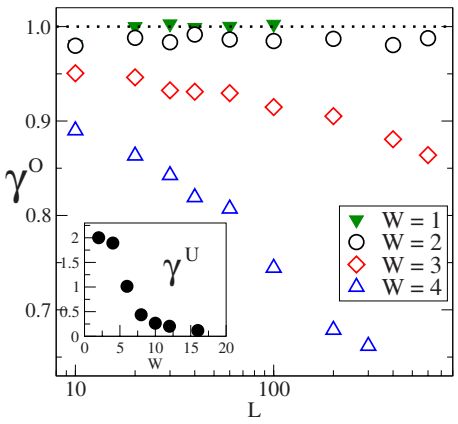

FIG. 5. (Color online) The size dependence of the parameter $\gamma^{\mathrm{O}}=2K_{12}^{\mathrm{O}}/K_{11}^{\mathrm{O}}$ for the 2D orthogonal model. We expect that γ^{O} decreases to zero for any value of the disorder W. However, the size of the system L is not sufficient to see this decrease when the disorder is small. Instead, we observe the diffusive limit $\gamma^{\mathrm{O}} \approx 1$. Only for sufficiently strong disorder, γ^{O} decreases to zero. In contrast to the symplectic model (Fig. 4) there is no indication for the existence of the critical point where γ^{O} converge to the L-independent limit. Inset shows the disorder dependence of γ^{U} for the unitary ensembles $(L=128,\ \alpha=1/8)$.

C. Critical regime (symplectic models)

Critical regime exists only for the S systems. In the critical regime, $W=W_c$ we found that both K_{11}^{S} and K_{12}^{S} decrease at the critical point to zero

$$K_{11}^{\mathrm{S}}(W=W_c), \quad K_{12}^{\mathrm{S}}(W=W_c) \propto \frac{1}{L} \tag{25}$$

(Fig. 3) so that γ^{S} reaches a critical value, $\gamma_c^{\mathrm{S}}=2K_{12}^{\mathrm{S}}/K_{11}^{\mathrm{S}}$ which does not depend on the size of the system

$$\gamma_c^{\mathrm{S}} = \mathrm{const.} \tag{26}$$

As shown in Fig. 3, the critical value γ_c^{S} is not universal but depend on the model. We obtain $\gamma^{\mathrm{S}}=2.601$ for the Ando model, and 1.795 for the Evangelou-Ziman model.

Figure 4 shows that the length and disorder dependence of parameter γ^{S} can be, at least, in principle, used for the estimation of critical parameters in the same way as mean conductance of the smallest Lyapunov exponent. For very weak disorder, we find that γ^{S} only weakly depends on the size of

the system and increases to the metallic limit $\gamma=4$ when L increases to infinity, indicating that the system is in the metallic regime. For stronger disorder, $\gamma^S \propto 1/L$ decreases to zero when the size of the system increases, in agreement with the prediction of the theory.[17] We found the critical regime between these to limits, where γ^S converges to the size-independent constant $\gamma_c^S \approx 2.60$ (obtained already in Fig. 3) when $W=W_c$.

For comparison, we show in Fig. 5 data for γ^O calculated for the 2D orthogonal model. We found no critical regime. Although $\gamma^O \approx 1$ for weak disorder, we expect that this is the finite-size effect, and γ^O will decrease to zero for each disorder strength when L increases.[8]

D. Universality

With two new parameters K_{11} and γ, we must verify if the transport properties of the system are still maintained by only a single parameter.[8] In the metallic regime, the answer is trivial since the entire matrix K reduces to model-independent numbers given by Eqs. (13), (15), and (19). The universality of the critical regime was shown in the previous section. Here, we concentrate on the localized regime, where we expect that K_{11} becomes an unambiguous function of the localization length.[20] The last can be estimated from the smallest parameter x_1,

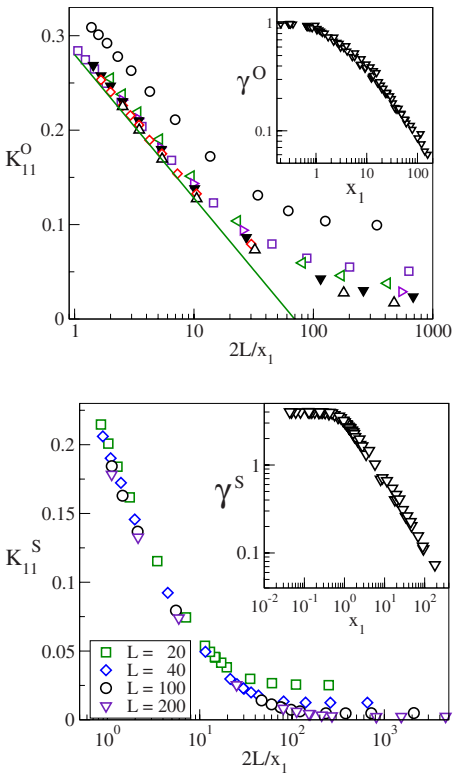

FIG. 6. (Color online) K_{11} as a function of the localization length ξ (estimated as $\xi=2L/x_1$) for the 2D orthogonal model (top) and the 2D symplectic model (bottom). The strength of the disorder varies between $W=1$ and $W=16$ in both figures. For strong disorder ($2L/x_1 \to 0$) data converge to the universal curve (solid line is a function $0.288-0.066$ ln ξ for the orthogonal model). Insets in both panels show that γ is an unambiguous function of x_1.

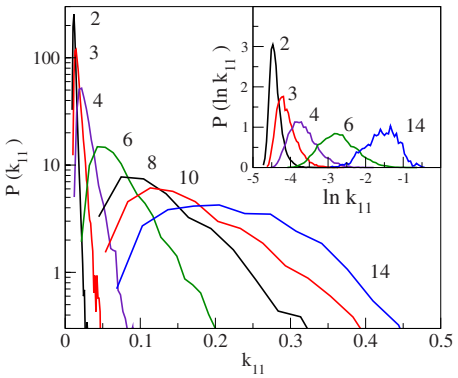

FIG. 7. (Color online) The probability distribution of k_{11} for the 2D orthogonal model with various disorder strength (given in the figure). The size of the system $L=200$. Inset shows the distributions $P(\ln K_{11})$. Data confirm that k_{11} is a good statistical variable with a well-defined mean value and variance.

$$\xi = \frac{2L}{x_1}. \tag{27}$$

In Fig. 6 we plot K_{11} as a function of ξ for the orthogonal and symplectic Ando models. Data confirm that the parameter K_{11} becomes a linear function of ln ξ with increasing system size and converge to the system-size-independent limit when $L \to \infty$.

Two insets of Fig. 6 show that the parameter γ is an unambiguous function of x_1 in all three regimes. In the localized regime, when $x_1 \sim L$, data confirm that $\gamma \sim 1/L$, consistent with prediction of the Muttalib's theory.

E. Statistical properties of k_{11}

In the previous analysis we dealt only with mean values of K_{11} and K_{12}. Since both k_{11} and k_{12} are statistical variables, we must also to study their statistical properties. Figure 7 shows the probability distribution of parameters k_{11} and ln k_{11} for the 2D orthogonal model. For each disorder, the mean value can be identified with the most probable value. In the localized limit, both K_{11} and Var k_{11} are of order of unity, and the distribution $P(k_{11})$ becomes size independent (Fig. 8).

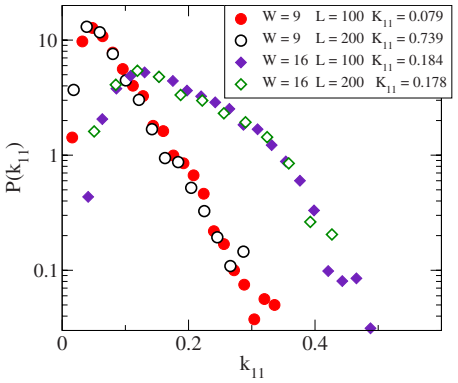

FIG. 8. (Color online) The probability distribution of k_{11} in the strongly localized regime for the Ando model. The mean value K_{11} is given in the legend.

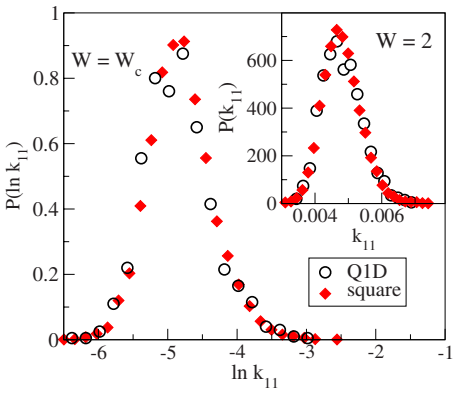

FIG. 9. (Color online) The probability distribution of k_{11} for the 2D Ando model at the critical point $W=W_c=5.525$ and in the metallic regime ($W=2$, inset). Both the square samples 100×100 and quasi one dimensional (Q1D) samples 100×5000 are considered.

In Fig. 9 we plot the probability distribution of k_{11} for the symplectic Ando model in the critical and metallic regimes. We demonstrate that the distributions for the square sample $L\times L$ with quasi-one-dimensional systems are almost identical.

F. Correlation g vs k_{11}

We have shown that $K_{11}\to0$ in the metallic regime but $K_{11}\sim O(1)$ in the insulator. Small values of K_{11} indicate that the mean conductance of the system is large. Contrary, large values of K_{11} correspond to systems with small mean conductance. This is in agreement with our expectation: small conductance means that the electron has problems to go through the sample. When it finally reaches the opposite side, its spatial distribution is not homogeneous any more.

However, the correspondence large k_{11}-small g holds only for mean values of these parameters. As shown in Fig. 10, the values of g and k_{11} for a given sample are not correlated within a given statistical ensemble: small values $g\ll\langle g\rangle$ can be accompanied with any value of k_{11}—either small $k_{11}\ll K_{11}$ or large $k_{11}\gg K_{11}$. The absence of the correlation, observed in both the metallic and in strongly localized regime, confirms that the statistical fluctuations of k_{11} do not affect the mean value of the conductance.

VI. CONCLUSION

The electron transport through disordered system is determined by spatial distribution of the electron inside the disordered sample, which can be measured by parameters K_{11} and γ. Our aim in this paper was to investigate how these two parameters depend on the size of the system, strength of the disorder and physical symmetry of the model. We concentrated on 2D disordered systems. In order to better understand the role of the disorder, we compare numerical data for the orthogonal and symplectic physical symmetry. For completeness, we add also a few data for the unitary ensemble.

In the diffusive regime, the size dependence of both parameters follows the analytical relations given by the theory

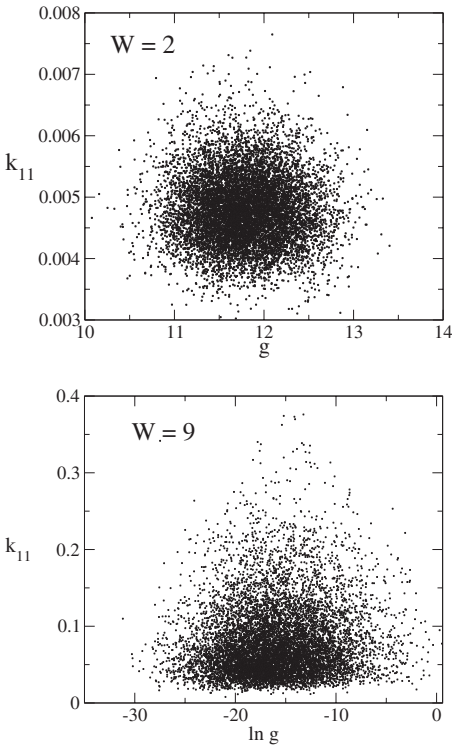

FIG. 10. 2D Ando model: k_{11} as a function of the conductance statistical ensemble of $N_{\mathrm{stat}}=10^4$ samples with disorder $W=2$ (top) and $W=9$ (bottom). The size of the system $L=100$.

of DMPK equation. In particular, γ equals to the symmetry parameter β. In the localized regime, K_{11} converges to the size-independent limit and $\gamma\sim1/L$.

For the symplectic models, which exhibit the metal-insulator transition, we analyze the size dependence of both parameters and we found that γ possesses a critical value γ_c when disorder $W=W_c$. Also, we found no significant difference between the values of K for the two-dimensional and quasi-one-dimensional systems. No critical value was found for the orthogonal model.

We also found that K_{11} is an unambiguous function of the localization length ξ and γ is uniquely given by the parameter x_1. Therefore, the use of these parameters does not contradict the single-parameter scaling theory.

Since the elements of matrices k are given by elements of statistical matrices v, they are also statistical variables. Fortunately, analysis of their probability distributions confirm that their mean values are good representatives of the statistical ensembles. We found no statistical correlations between the conductance and k_{11}. Therefore, we conclude that mean values, K_{11} and K_{12}, and, consequently, $\gamma=2K_{12}/K_{11}$, are physical parameters for the description of disordered systems.

ACKNOWLEDGMENTS

This work was supported by Project VEGA under Grant No. 0633/09.

[1] P. A. Lee and T. V. Ramakrishnan, Rev. Mod. Phys. **57**, 287 (1985).
[2] B. Kramer and A. MacKinnon, Rep. Prog. Phys. **56**, 1469 (1993).
[3] P. W. Anderson, Phys. Rev. **109**, 1492 (1958).
[4] O. N. Dorokhov, JETP Lett. **36**, 318 (1982); P. A. Mello, P. Pereyra, and N. Kumar, Ann. Phys. (N.Y.) **181**, 290 (1988).
[5] B. L. Altshuler, JETP Lett. **41**, 648 (1985); P. A. Lee and A. D. Stone, Phys. Rev. Lett. **55**, 1622 (1985).
[6] J.-L. Pichard, in *Quantum Coherence in Mesoscopic Systems*, NATO ASI Series Vol. 254, edited by B. Kramer (Plenum Press, New York, London, 1991).
[7] C. W. J. Beenakker, Rev. Mod. Phys. **69**, 731 (1997); C. W. J. Beenakker and B. Rajaei, Phys. Rev. Lett. **71**, 3689 (1993); Phys. Rev. B **49**, 7499 (1994).
[8] E. Abrahams, P. W. Anderson, D. C. Licciardello, and T. V. Ramakrishnan, Phys. Rev. Lett. **42**, 673 (1979); A. MacKinnon and B. Kramer, *ibid.* **47**, 1546 (1981).
[9] F. Evers and A. Mirlin, Rev. Mod. Phys. **80**, 1355 (2008).
[10] A. M. Somoza, M. Ortuno, and J. Prior, Phys. Rev. Lett. **99**, 116602 (2007).
[11] A. M. García-García, Phys. Rev. Lett. **100**, 076404 (2008).
[12] P. Markoš, Phys. Rev. B **65**, 104207 (2002).
[13] P. Markoš, Acta Phys. Slov. **56**, 561 (2006).
[14] J. Prior, A. M. Somoza, and M. Ortuno, Eur. Phys. J. B **70**, 513 (2009).
[15] A. M. Somoza, J. Prior, M. Ortuno, and I. V. Lerner, Phys. Rev. B **80**, 212201 (2009).
[16] Z. Qiao, Y. Xing, and J. Wang, Phys. Rev. B **81**, 085114 (2010).
[17] K. A. Muttalib and J. R. Klauder, Phys. Rev. Lett. **82**, 4272 (1999). In this paper, Eq. 4 was derived for the orthogonal symmetry class. We found that it has the same form also for the unitary and symplectic classes.
[18] P. Markoš, Physica B **405**, 3029 (2010).
[19] P. Markoš, K. A. Muttalib, P. Wölfle, and J. R. Klauder, Europhys. Lett. **68**, 867 (2004).
[20] K. A. Muttalib, P. Markoš, and P. Wölfle, Phys. Rev. B **72**, 125317 (2005).
[21] A. Douglas and K. A. Muttalib, Phys. Rev. B **80**, 161102 (2009).
[22] J. Brndiar, R. Derian, and P. Markoš, Phys. Rev. B **76**, 155320 (2007).
[23] S. N. Evangelou and T. Ziman, J. Phys. C **20**, L235 (1987).
[24] T. Ando, Phys. Rev. B **40**, 5325 (1989).
[25] P. A. Mello and J.-L. Pichard, Phys. Rev. B **40**, 5276 (1989).
[26] E. N. Economou and C. M. Soukoulis, Phys. Rev. Lett. **46**, 618 (1981); **47**, 973 (1981).
[27] In the absence of the disorder, the z component of the wave vector

$$\cos k_z a = \frac{1}{2V_\parallel}[E - 2V_\perp \cos k_x a]$$

is real for all possible values of k_x provided that the energy E is close to the band center $E=0$.
[28] P. Markoš and L. Schweitzer, J. Phys. A **39**, 3221 (2006).
[29] A. M. S. Macêdo and J. T. Chalker, Phys. Rev. B **46**, 14985 (1992).
[30] P. A. Mello, J. Phys. A **23**, 4061 (1990).
[31] For symplectic models, each element of M and M_0 is the 2×2 matrix.
[32] J. B. Pendry, A. MacKinnon, and P. J. Roberts, Proc. R. Soc. London, Ser. A **437**, 67 (1992).